Journal of Biomolecular NMR, **21:** 191–208, 2001.
KLUWER/ESCOM

Membrane-bound structure and alignment of the antimicrobial β-sheet peptide gramicidin S derived from angular and distance constraints by solid state ^{19}F-NMR

Jesús Salgado[a,#], Stephan L. Grage[a,§], Leslie H. Kondejewski[c,$], Robert S. Hodges[b,c,‡], Ronald N. McElhaney[b,c] & Anne S. Ulrich[a,*]

[a]*Department of Molecular Biology, University of Jena, Winzerlaer Str. 10, 07745 Jena, Germany;* [b]*Department of Biochemistry, University of Alberta, Edmonton, Alberta T6G 2H7, Canada;* [c]*Protein Engineering Network of Centres of Excellence, University of Alberta, Edmonton, Alberta T6G 2S2, Canada; New addresses:* [§]*Department of Biochemistry, South Parks Road, Oxford OX1 3QU, England;* [#]*Department of Biochemistry and Molecular Biology, Dr. Moliner 50, 46100 Burjassot, Valencia, Spain;* [$]*Caprion Pharmaceuticals Inc., 7150 Alexander-Flemming, St. Laurent, Quebec H4S 2C8, Canada;* [‡]*University of Colorado Health Sciences Center, 4200 E. Ninth Avenue, Denver, Colorado 80262, U.S.A.*

Received 26 April 2001; Accepted 28 August 2001

Key words: amphiphilic antimicrobial peptide, chemical shift anisotropy, CPMG multipulse experiment, cyclic beta-sheet peptide, distance measurement, fluorine-labelling, 4-fluoro-phenylglycine, homonuclear dipolar coupling, macroscopically aligned membrane sample, segmental orientation

Abstract

The antimicrobial properties of the cyclic β-sheet peptide gramicidin S are attributed to its destabilizing effect on lipid membranes. Here we present the membrane-bound structure and alignment of a derivative of this peptide, based on angular and distance constraints. Solid-state ^{19}F-NMR was used to study a ^{19}F-labelled gramicidin S analogue in dimyristoylphosphatidylcholine bilayers at a lipid:peptide ratio of 80:1 and above. Two equivalent leucine side chains were replaced by the non-natural amino acid 4F-phenylglycine, which serves as a highly sensitive reporter on the structure and dynamics of the peptide backbone. Using a modified CPMG multipulse sequence, the distance between the two ^{19}F-labels was measured from their homonuclear dipolar coupling as 6 Å, in good agreement with the known backbone structure of natural gramicidin S in solution. By analyzing the anisotropic chemical shift of the ^{19}F-labels in macroscopically oriented membrane samples, we determined the alignment of the peptide in the bilayer and described its temperature-dependent mobility. In the gel phase, the ^{19}F-labelled gramicidin S is aligned symmetrically with respect to the membrane normal, i.e., with its cyclic β-sheet backbone lying flat in the plane of the bilayer, which is fully consistent with its amphiphilic character. Upon raising the temperature to the liquid crystalline state, a considerable narrowing of the ^{19}F-NMR chemical shift dispersion is observed, which is attributed the onset of global rotation of the peptide and further wobbling motions. This study demonstrates the potential of the ^{19}F nucleus to describe suitably labelled polypeptides in membranes, requiring only little material and short NMR acquisition times.

*To whom correspondence should be addressed.
E-mail: ulrich@molebio.uni-jena.de

Abbreviations: ^{19}F-NMR, fluorine nuclear magnetic resonance; 4F-Phg, 4-fluoro-phenylglycine; $\mathbf{B_0}$, static magnetic field direction; C_2, symmetry axis of the gramicidin S molecule; CPMG, Carr–Purcell–Meiboom–Gill multipulse sequence; CSA, chemical shift aisotropy; DMPC, dimyristoyl-phosphatidylcholine; F-GS, ^{19}F-labelled gramicidin S with 4F-Phg in positions 3 and 8; F-GS(KY), hypothetical ^{19}F-labelled analogue of GS(KY); GS, gramicidin S; GS(KY), gramicidin S analogue with Orn→Lys and Phe→Tyr substitutions; MAS, magic angle spinning; **N**, macroscopic sample normal; r, distance between two ^{19}F-labels; S_{mol}, molecular order parameter; α,β, Euler angles; δ_{11}, δ_{22}, δ_{33}, principal values of a non-axially symmetric CSA tensor; $\delta_{\perp}$, $\delta_{||}$, principal values of an axially averaged CSA tensor; δ_{iso}, isotropic chemical shift value; $\delta(\alpha,\beta)$, resonance frequency corresponding to any particular CSA tensor orientation as a function of the Euler angles; δ^0, resonance frequency of an oriented sample observed at the horizontal sample alignment; δ^θ, resonance frequency observed of an oriented sample with axial symmetry at any sample tilt angle τ; Δ_{CSA}, width of the chemical shift anisotropy; Δ_{FF}, homonuclear dipolar coupling between two ^{19}F-labels; η, angle between the C_α-C_β bond of 4F-Phg and the symmetry axis of the F-GS molecule; ϕ,ψ, backbone torsion angles; ρ, angle used to relate α with χ_1 (see Figure 3B); $\sigma(t)$, time-dependent angle between the molecular symmetry axis of F-GS and the membrane normal; θ, angle between the internuclear ^{19}F-^{19}F vector and the magnetic field direction $\mathbf{B_0}$; τ, macroscopic sample tilt, defined as the angle between the membrane normal **N** and the magnetic field direction $\mathbf{B_0}$; χ_1, side chain torsion angle around C_α-C_β.

Introduction

Membrane-associated peptides and proteins are one of the major challenges to modern structural biology, as the presence of the lipid bilayer imposes fundamental limitations on the techniques available for structural studies. Among these techniques, solid state NMR is particularly promising, because membrane proteins can be studied in their natural lipid environment and at conditions close to physiological (Losonczi et al., 2000; Fu and Cross, 1999; Davis and Auger, 1999; Bechinger, 1999; Marassi and Opella, 1998; Smith et al., 1996; Watts et al., 1995). Different solid state NMR strategies are available which usually involve either uniaxial orientation of the sample (Losonczi et al, 2000; Marassi and Opella, 1998; Losonczi and Prestegard, 1998; Fu and Cross, 1999) or magic-angle spinning (MAS) (DeGroot, 2000; Davis and Auger, 1999; Smith et al., 1996), and each approach may be combined with various recoupling schemes and sophisticated multidimensional pulse sequences (van Beek et al., 2000; Gu and Opella, 1999; Ramamoorthy et al., 1999; van Rossum et al., 1997). The analysis of anisotropic spin interactions in oriented samples is rather straightforward in the case of membrane proteins, given the intrinsic two-dimensional nature of the lipid bilayer (Gröbner et al., 2000; Fu and Cross, 1999; Opella et al., 1999; Bechinger, 1999; Marassi and Opella, 1998; Ulrich et al., 1994, 1995).

A significant limitation to many solid state NMR studies in biological systems is the use of isotope labels that possess an intrinsically low sensitivity, such as ^{15}N, ^{2}H or ^{13}C. As an alternative, we are exploring the potential of fluorine as a selective label (Grage et al., 2000, 2001a; Grage and Ulrich, 1999, 2000), because ^{19}F-NMR is several orders of magnitude more sensitive in terms of measurement time, and it does not suffer from any background signals in biological samples (Ulrich, 2000; Goetz et al., 1999; Harris and Jackson, 1991; Miller, 1996). Especially when working with small amounts of material, with very large proteins, or at low peptide concentrations in the membrane, ^{19}F-NMR can yield structural parameters about systems that would otherwise not be accessible to solid state NMR. The broad chemical shift anisotropy (CSA) of ^{19}F is highly informative with respect to orientational constraints, and ^{19}F also engages in strong dipolar couplings which are useful for measuring long-range dipolar interactions as a basis for distance constraints (Grage and Ulrich, 1999, 2000; Gilchrist et al., 2001). Selective ^{19}F-labels can be readily introduced into aromatic or aliphatic side chains, usually with little or no effect on the conformation and functional properties of the protein (Gerig, 1994, 1998; Danielson and Falke, 1996).

Here, we describe the interaction of a ^{19}F-labelled gramicidin S analogue (F-GS) with phospholipid bilayers, as an example to illustrate a novel solid state ^{19}F-NMR strategy for studying biologically active peptides in membranes. Gramicidin S (GS) is a cationic decapeptide from *Bacillus brevis* with the symmetric sequence cyclic-(Val-Orn-Leu-DPhe-Pro)$_2$. It exhibits antimicrobial activity against a broad spectrum of Gram-negative and Gram-positive bac-

teria and several fungi, and it also possesses some hemolytic activity (McInnes et al., 2000; Kondejewski et al., 1996a, b). The structure of GS is known from X-ray crystallography (Hull et al., 1978) as well as from ^{1}H-NMR studies in a number of different solvents (Gibbs et al., 1998; Xu et al., 1995). Its antiparallel β-sheet conformation possesses a twofold symmetry, in which two equivalent short strands are connected by β-turns consisting of the D-Phe and Pro residues. The molecule has a pronounced amphiphilic character, since the positively charged ornithine (Orn) side chains are located on one face of the cyclic β-sheet, while the hydrophobic side chains of Val, Leu and Pro point towards the opposite side (Xu et al., 1995; Hull et al., 1978). Just as in the case of other amphiphilic peptide antibiotics (Bechinger, 1999; Sitaram and Nagaraj, 1999), it is generally accepted that the site of action of GS is the plasma membrane of the target cell (Prenner et al., 1999). GS shows a high affinity for a wide variety of natural and synthetic lipid bilayers with different head groups and different viscous properties (Prenner et al., 1997, 1999). Binding of the peptide leads to moderate shifts and a considerable broadening of the main lipid phase transition (Prenner et al., 1999), and it increases the membrane permeability for ions and small metabolites in a concentration-dependent manner (Wu et al., 1999).

It has been suggested from ^{2}H-NMR (Datema et al., 1986) and FT-IR measurements (Lewis et al., 1999) that GS resides near the glycerol backbone of the lipid bilayer, such that its positively charged ornithine residues can interact with the polar headgroups, while the hydrophobic residues penetrate the upper region of the hydrocarbon chains. This topology is in agreement with a recent molecular dynamics similation which also proposes that GS lies flat in the membrane (Mihailescu and Smith, 2000). However, no direct experimental evidence has been published so far on the structure and alignment of the peptide in lipid bilayers, which is a crucial aspect for interpreting its mechanism of membrane destabilization. Here we address these questions through the direct observation of a ^{19}F-labelled derivative of GS in dimyristoylphosphatidylcholine (DMPC) bilayers by solid state ^{19}F-NMR. To determine the overall conformation, the orientation, and the mobility of the cyclic F-GS peptide in the lipid bilayer, two equivalent hydrophobic side chains were substituted by 4F-phenylglycine (4F-Phg). This non-natural amino acid was selected here – for the first time – as a probe for addressing the behaviour of any rigid secondary structure element, because the fluorinated phenyl ring protrudes stiffly from the peptide backbone. Distance constraints can thus be readily determined in relation to the peptide backbone using a static CPMG experiment (Grage and Ulrich, 1999, 2000), and the orientation of the non-axially symmetric ^{19}F CSA tensor in the membrane can be evaluated using macroscopically oriented NMR samples (Grage and Ulrich, 2001a; Grage et al., 2001b; Ulrich and Watts, 1993). For a self-consistent structure analysis of the membrane-bound gramicidin S derivative, several structural parameters have to be either directly measured, or they have to be first assumed and subsequently confirmed experimentally. These parameters include: i) the overall backbone conformation taken from the ^{1}H-NMR structure of natural GS in solution and verified here independently by a ^{19}F-^{19}F distance measurement; ii) the side chain torsion angle χ_1 of 4F-Phg, accessible from energy minimization and independently verified here by analyzing the ^{19}F CSA tensor alignment; and iii) the molecular order parameter S_{mol} of the peptide, deduced here from the narrowing of the ^{19}F chemical shift dispersion. The overall conformation, alignment, and dynamics of FGS in DMPC bilayers has thus been characterized over a range of different conditions by means of highly sensitive, static ^{19}F-NMR measurements.

Materials and methods

Preparation of fluorine-labelled gramicidin S

The ^{19}F-labelled GS peptide was prepared by automated *t*-butyloxycarbonyl chemistry, the crude peptide cleaved from the resin, purified by reversed-phase HPLC, cyclized, and re-purified by reversed-phase HPLC, as reported (Kondejewski et al., 1996). To replace each of the two naturally occurring leucine residues of GS (Leu3 and Leu8) by 4F-Phg, a racemic 4F-DL-Phg mixture (Fluka) was used for each of the corresponding coupling steps. The resulting mixture of cyclic peptide diastereomers was resolved and purified by reversed-phase HPLC. The desired product (containing two 4F-L-Phg residues) exhibited the greatest retention time due to the formation of the largest hydrophobic binding domain (Kondejewski et al., 1999). The sample obtained that way contains significant amounts of trifluoroacetic acid from the HPLC purification buffers, which was removed by ion exchange chromatography using amberlite resin (Merck). The quality of the purified F-GS was

assessed by ^{19}F-NMR in aqueous solution, where a single resonance was observed for the L,L-diastereomer of 4F-Phg while the D,L-diastereomer gave rise to two peaks due to the inequivalence of the two 4F-Phg substituents.

Antimicrobial activity

The antimicrobial activity of the ^{19}F-labelled F-GS peptide was compared to that of natural GS (Sigma, St. Louis, MO) as described (McInnes et al., 2000). Peptides dissolved in Mueller Hinton broth were mixed with molten agarose, the solution allowed to solidify in microtiter plates, and test strains were applied to the agarose. Minimal inhibitory concentrations were determined as the concentration of peptide required to completely inhibit growth of a given microorganism after 24 h.

Sample preparation

Samples for solid state ^{19}F-NMR measurements typically contained 22.5 mg DMPC (Avanti Polar Lipids, Alabaster, AL) and either 0.5 mg F-GS (lipid:peptide molar ratio of 80:1) or 0.2 mg F-GS (200:1). For the non-oriented powder samples, lipid-peptide mixtures were dissolved in chloroform:methanol (80:20) and dried, first with a stream of N_2 and then under vacuum for at least 4 h. The dried material was hydrated for 24 h at 98% humidity and 42 °C over a saturated solution of $(NH_4)_2SO_4$ and subsequently sealed in small plastic bags. To prepare macroscopically oriented samples, the lipid-peptide mixtures were dissolved in 450 µl chloroform:methanol (80:20), spread as 30 µl aliquots onto glass plates (12 mm × 7.5 mm × 0.06 mm) and dried, first in air and then under vacuum for at least 4 h. Fifteen dried glass plates were stacked, hydrated at 98% humidity and 42 °C for at least 24 h, and wrapped in parafilm and plastic foil. The quality of orientation of the membranes was assessed by ^{31}P-NMR and all samples used in this study were well-oriented to at least 80% as judged by simulation of these spectra (Ulrich et al., 1992). Any remaining powder contributions were subtracted from the experimental data, and a broad background signal arising from the ^{19}F-NMR probe was also removed.

NMR experiments

All NMR data were acquired in a widebore magnet at 11.74 T (500 MHz for ^{1}H) with a Varian Unity Inova spectrometer. ^{19}F-NMR spectra were recorded at 470.3 MHz with a double-resonance ^{1}H/^{19}F variable-angle flat-coil (9 mm × 2.5 mm × 10 mm) probe (Doty Scientific, Columbia, SC), using a Hahn-echo sequence with 2.2 µs pulse length, 25 µs echo delay, 2.4 s relaxation delay, 10 ms acquisition time, and 25 kHz ^{1}H-decoupling during acquisition. In the fluid phase of the lipids, spectra consisted of 2000 scans (1.3 hours experiment time) and FID were processed using a 20 Hz exponential linebroadening function. In the gel state, 10 000 scans were recorded (6.5 h experiment time) and spectra were processed with 500 Hz exponential linebroadening.

The ^{19}F dipolar spectra were obtained using a CPMG multipulse sequence, modified with an xy8 phase cycle, using mid-to-mid pulse spacings of 48 µs over a duration of 100 ms, without ^{1}H-decoupling (Grage and Ulrich, 1999, 2000). The echos were acquired in the windows between the composite π pulses (90_x-180_y-90_x) with a dwell time of 1 µs/point. Up to 4 raw data points at the echo top were averaged and an FID analogue was composed from these averaged echo amplitudes. 3200 transients were accumulated for the oriented sample in a horizontal alignment ($\tau = 0°$). The phase alternation of the magnetization in the successive windows was taken into account by software manipulation, and the FID analogue was converted into the dipolar spectrum via Fourier Transformation. A linebroadening of 10 Hz was applied. The spectrum was laterally scaled according to the extrapolated dipolar splitting at a duty cycle of 0% (Grage et al., 2000), after having established that different CPMG window lengths yielded a linear correlation between the splitting and the duty cycle (measured between 12% and 20%).

Circular dichroism experiments

CD spectra were recorded at 25 °C on a Jasco J-720 spectropolarimeter using 2-mm path length quartz cuvettes. Averages of four scans were collected at 0.2 nm intervals between 190 nm and 250 nm. The peptides were dissolved at 0.1 mg/ml in 10 mM sodium acetate buffer at pH 5.6, and a stock suspension of DMPC small unilamellar vesicles in water was prepared by sonication. Samples with a lipid:peptide mixture (80:1 molar ratio) were obtained by mixing the appropriate amounts of GS (or F-GS) and DMPC from the respective stock solutions.

Molecular modelling

Model structures of the gramicidin derivatives were built using the *Discover* and *Search-Compare* modules of the *InsightII* software package and the *cvff-2.3* forcefields (Molecular Simulations, Inc., San Diego, CA). The structure of the ^{19}F-labelled analogue was based on the coordinates of natural GS as determined from ^{1}H-NMR NOE constraints (Xu et al., 1995), which are consistent with molecular dynamics calculations in a lipid bilayer (Mihailescu and Smith, 1999, 2000). To create a model structure of F-GS, we built as a first step a 4F-Phg fragment using standard crystallographic atomic distances and angles, and energy minimization. Two 4F-Phg side chains were then attached to GS in place of the two naturally occurring Leu residues at positions 3 and 8, maintaining the same backbone structure as natural GS. The preferred side-chain torsion angle of 4F-Phg was evaluated independently by a systematic conformational search based on the N-acetyl-N′-methylamide dipeptide derivative of this residue as a model compound. The most favourable torsion angle was then used in the model of F-GS. The reported conformations of the Val, Orn, D-Phe and Pro residues in natural GS were kept unchanged, as they were found to be sterically compatible with the conformation chosen for the 4F-Phg residues.

Results and discussion

^{19}F-labelling strategy with 4F-phenylglycine

The key aspect of this study is the use of ^{19}F as a highly sensitive nucleus to probe by solid state NMR the structure, alignment, and dynamics of an amphiphilic peptide bound to a lipid membrane. As a general strategy, we propose to introduce a selective ^{19}F-label into a peptide by substituting a hydrophobic side chain with 4F-phenylglycine. This non-natural amino acid is particularly suitable for structural studies, because the position of the ^{19}F-nucleus is well-defined with respect to the peptide backbone. The straight connection across the rigid aromatic ring makes it possible to correlate the orientation of the ^{19}F CSA tensor with the orientation of the C_α–C_β bond of 4F-Phg. It is thus possible to measure a local structural constraint on the peptide backbone, which may then be used to define the overall orientation of a given secondary structure element.

Biological activity of the ^{19}F-labelled GS

It has been previously shown that the main factors governing the membrane interactions of GS and its antimicrobial activity are the net charge and the amphiphilic nature of the peptide (Prenner et al., 1997; Kondejewski et al., 1999). In this sense, the replacement of the two Leu residues by two 4F-Phg side chains is considered to be a conservative modification, since the distribution of the positively charged side chains (Orn) and the hydrophobic residues on opposite sides of the β-sheet remains unchanged. The biological consequences of the Leu by 4F-Phg substitution were examined by testing the antimicrobial activity of F-GS against a number of different Gram-negative and Gram-positive bacteria. The Minimum Inhibitory Concentrations (MIC) were determined from a series of 2-fold dilutions for 12 different strains, each of which yielded the same concentrations for GS and F-GS within a factor of two, as summarized in Table 1. Within this accuracy and over the wide range of microorganisms tested, we consider the activity of the modified F-GS to be virtually identical to that of natural GS, thus supporting the essentially non-perturbing nature of 4F-Phg and the biological relevance of our structural studies.

Backbone conformation of the ^{19}F-labelled GS

The antiparallel β-sheet structure of GS is well known from previous X-ray studies on a hydrated urea complex (Hull et al., 1978) and from ^{1}H-NMR studies in solution (Xu et al., 1995, Gibbs et al., 1998). The backbone structure is schematically represented in Figure 1, together with a model structure of F-GS. This model was constructed on the assumption that the backbone conformation does not change significantly upon Leu by 4F-Phg substitution, and that it remains the same in solution as in the membrane-bound state. We support this assumption by two pieces of evidence, based on circular dichroism (CD) spectroscopy and on an intramolecular distance measurement by solid state ^{19}F-NMR.

Figure 2 shows that GS gives rise to essentially the same characteristic CD spectrum in water as it does in sonicated lipid vesicles, with minima at around 208 nm and 218 nm (Figure 2A). The corresponding spectra of F-GS (Figure 2B) show comparable features with only small changes in the position and ellipticity of the bands. We note that the substitution of two aliphatic side chains by aromatic residues is expected to cause slight differences in the spec-

Table 1. Antimicrobial activity of GS and F-GS

Microorganism		Minimal inhibitory concentration (μg/ml)	
		GS	F-GS
Gram negative	*A. calcoaceticus*	8	4
	E. cloacae	32	32
	E. coli	16	32
	K. pneumoniae	16	16
	P. aeruginosa	32	64
	S. maltophilia	8	8
Gram positive	*E. faecalis*	2	4
	S. aureus	2	2
	S. epidermidis	2	2
	S. mitis	0.5	2
	S. pneumoniae	1	2
	S. pyrogenes	0.5	1

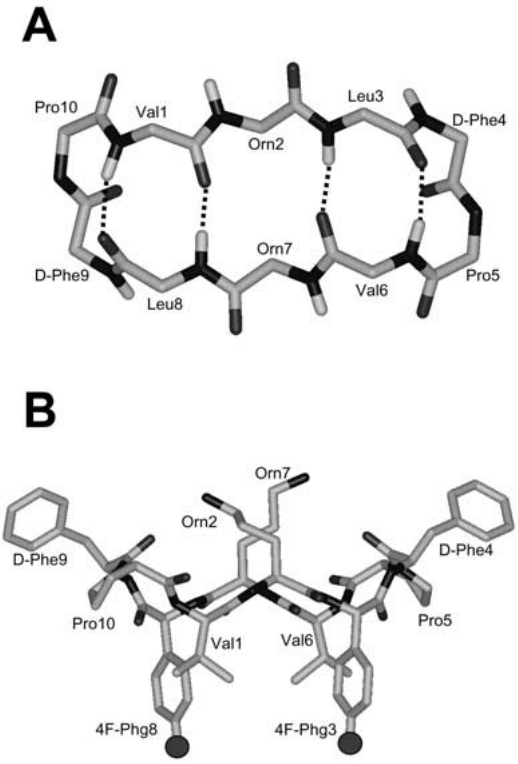

Figure 1. Model of gramicidin S based on the high resolution ^{1}H-NMR structure of the naturally occurring peptide in DMSO (Xu et al., 1995). The backbone structure of the wild type peptide GS (A) was used to model the ^{19}F-labelled analogue F-GS (B), by replacing the two original Leu side chains by 4F-phenylglycine.

tra of this 10-residue peptide, because the aromatic rings contribute to the absorption (Kahn, 1979; Adler et al., 1973). Nevertheless, the CD data indicate that both F-GS and natural GS exhibit very similar backbone structures, which do not depend appreciably on the presence of lipids. This observation is in agreement with molecular dynamics calculations (Mihailescu and Smith, 1999, 2000) and structural studies, where GS was found to maintain its conformation in a number of different environments with varying polarity and hydrogen-bonding potential, including water, methanol, ethanol, dimethyl sulfoxide, detergent micelles and phospholipid bilayers (Waki et al., 1970).

Intramolecular distance measurement by solid state ^{19}F-NMR

It has been shown that the overall tendency of various GS analogues to assume a stable cyclic β-sheet structure depends (periodically) on the number of residues forming the paired strands rather than on the specific sequence, provided that the essential D-Phe (or D-Tyr) and Pro residues are conserved in the turns (Gibbs et al., 1998). Nevertheless, a comparison of published ^{1}H-NMR structures in solution demonstrates that the detailed backbone conformation of a conservatively modified gramicidin analogue GS(KY) [cyclic-(Val-Lys-Leu-DTyr-Pro)$_2$] (Gibbs et al., 1998) differs significantly from that of the native peptide [cyclic-(Val-Orn-Leu-DPhe-Pro)$_2$] (Xu et al., 1995). In Figure 3, the two different coordinate sets of native

GS and its analogue GS(KY) were used to generate two alternative models for F-GS by replacing the Leu side-chains with 4F-phenyl rings while keeping the corresponding backbones intact. The dramatic effect of slight changes in the backbone torsion angles on the orientation of the ^{19}F-labelled side chains had to be very critically evaluated, especially in view of the fact that any small deviations in our starting model might lead to considerable errors in the analysis of the solid state ^{19}F-NMR data. To circumvent these ambiguities, we verified the F-GS coordinates by measuring the distance between the two ^{19}F-labels, which will be illustrated only qualitatively at this point, and then evaluated quantitatively further below.

Based on the native peptide backbone structure, the expected ^{19}F-^{19}F distance in the F-GS model (Figure 3A) is evaluated as 7.3 Å, whereas it would correspond to 13.5 Å in the F-GS(KY) analogue (Figure 3B). Experimentally, the distance r between two ^{19}F-labels can be determined by solid state NMR from their homonuclear dipolar coupling, which is comparatively long-range and thereby highly informative for this particular nucleus (Grage and Ulrich, 1999, 2000). The ^{19}F homonuclear dipolar coupling, Δ_{FF} (in Hz), is related to the distance, r (in Å), by the following equation

$$[\Delta_{FF}/\mathrm{Hz}] = 318360[r/\text{Å}]^{-3}(3\cos^2\theta - 1)/2, \quad (1)$$

where θ is the angle between the internuclear ^{19}F-^{19}F vector and the magnetic field direction $\mathbf{B_0}$, and the numerical factor is derived from some natural constants and the gyromagnetic ratios of ^{1}H and ^{19}F (Grage and Ulrich, 1999). The maximum dipolar splitting is reached for the case of $\theta = 0°$ and when there is no motional averaging, otherwise the observed couplings are reduced (see the order parameter analysis below). According to Equation 1, a distance of 7.3 Å as in the F-GS model would correspond to a maximum dipolar coupling of 790 Hz, whereas a distance of 13.5 Å as in the F-GS(KY) model would be consistent with a coupling of no more than 130 Hz.

For measuring the intramolecular dipolar coupling within F-GS, we have recently described an experiment that is suitable for static oriented membrane samples (Grage and Ulrich, 1999, 2000). Without any need for magic angle spinning or ^{1}H-decoupling, pure dipolar ^{19}F-spectra can be obtained using a modified CPMG multipulse sequence which is improved by phase cycling and composite pulses. Figure 3C shows the CPMG spectrum of F-GS in DMPC at a lipid:peptide ratio of 80:1 and a temperature of 30 °C, corresponding to the liquid crystalline state of the membrane. A dipolar splitting $\Delta_{FF} = 270$ Hz is clearly resolved in this oriented sample, which was placed with its normal parallel to the magnetic field $\mathbf{B_0}$. Note that oriented membranes, as opposed to non-oriented dispersions, not only provide an improved resolution in the dipolar spectra, but they also contain valuable angular information about the alignment θ of the internuclear vector, as will be discussed below (Grage and Ulrich, 1999, 2000; Grage et al., 2000). The important conclusion to be drawn at this point is that the observed splitting of 270 Hz is significantly larger than the maximum splitting of 130 Hz that would be compatible with the hypothetical structure of the gramicidin F-GS(KY) analogue. Therefore, we can exclude the possibility that our ^{19}F-labelled gramicidin S assumes a distorted structure resembling GS(KY). The fact that 270 Hz is smaller than the maximum 790 Hz for natural GS is of no concern, as the reduction can be explained by motional averaging. We will demonstrate quantitatively below that F-GS indeed possesses a backbone conformation that is close to the native structure of GS (Figure 3A). For now, we will base our model structure of F-GS on the coordinates of natural GS, which were determined by ^{1}H NMR in solution (Xu et al., 1995). Recently, it has been reported from molecular dynamics calculations that this structure remains essentially the same in a lipidic environment (Mihailescu and Smith, 2000).

Theoretical considerations for the ^{19}F CSA tensor analysis

The anisotropy of the ^{19}F CSA tensor of a 4F-Phg residue carries fundamental structural information about the side chain orientation and dynamics, and in favourable cases also about the peptide backbone to which it is connected. This information can be extracted from solid state ^{19}F-NMR spectra of the polypeptide in oriented membrane samples. Before proceeding with an interpretation of the experimental ^{19}F-NMR data, consider first the characteristics of the fluorine CSA tensor in a 4F-phenyl ring and its alignment in the framework of a F-GS molecule interacting with an oriented lipid bilayer. In contrast to previous studies of oriented biological samples making use of the axially symmetric ^{2}H quadrupolar interaction (Gröbner et al., 2000; Ulrich et al., 1994, 1995; Ulrich and Watts, 1993) or the (near-)axially symmetric ^{15}N CSA and dipolar tensors (Marassi and Opella, 1998; Fu and Cross, 1999; Gu and Opella, 1999; Ramamoor-

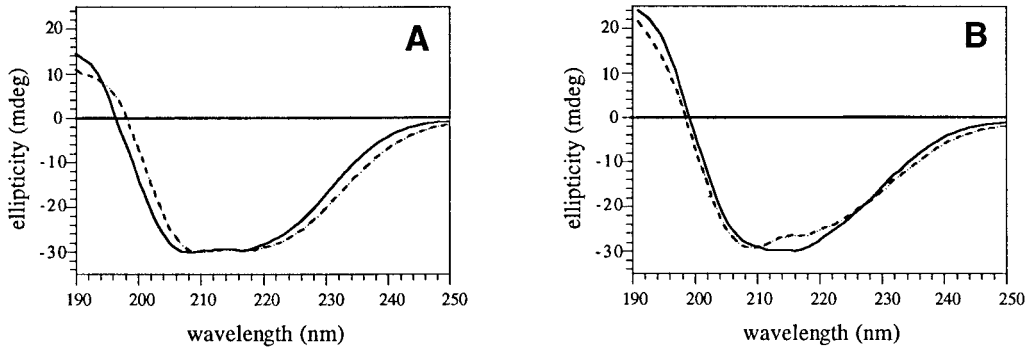

Figure 2. Circular dichroism spectra of GS (A) and F-GS (B) in H_2O (—) and in the presence of sonicated DMPC vesicles (- - -).

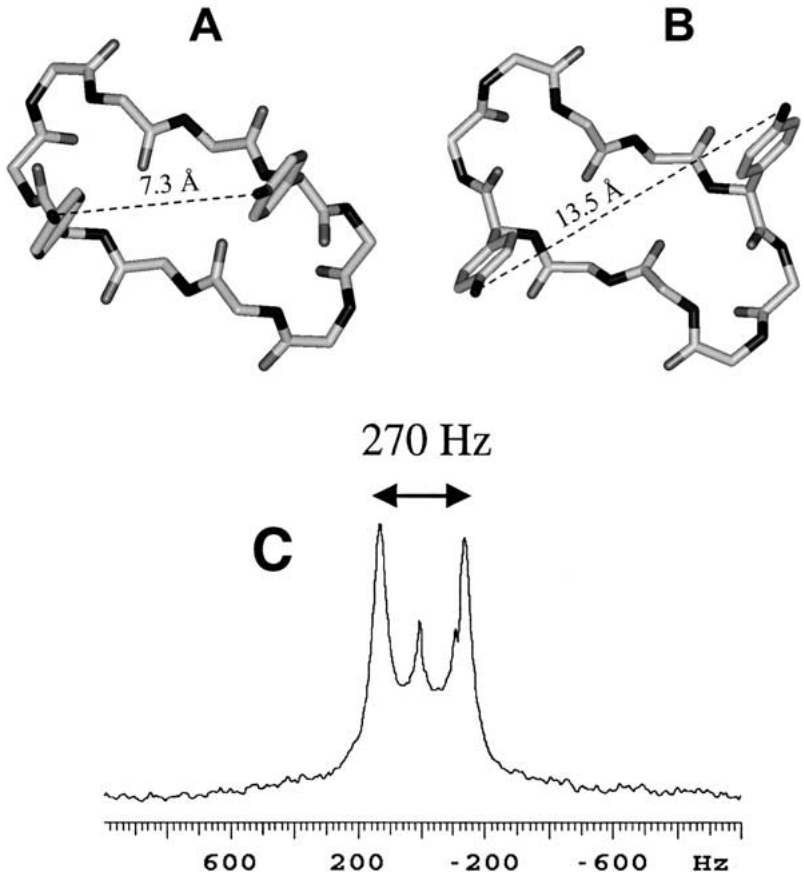

Figure 3. ^{19}F-^{19}F distance in 4F-Phg-labelled GS derivatives, and the corresponding experimental ^{19}F-^{19}F dipolar coupling in F-GS in DMPC bilayers. In a model structure of F-GS (A), constructed from the coordinates of the native peptide in solution, the intramolecular ^{19}F-^{19}F distance corresponds to 7.3 Å. For comparison, the backbone conformation of a conservatively modified peptide GS(KY) was used to build the analogous F-GS(KY) (B). The internuclear distance corresponding to F-GS in DMPC is experimentally accessible from the well-resolved dipolar splitting in a CPMG ^{19}F NMR spectrum (C) measured for a horizontally aligned sample at 30 °C.

thy et al., 1999; Opella et al., 1999; Bechinger, 1999), the ^{19}F CSA is highly non-axially-symmetric and thereby offers a higher information content, provided that the redundancy of similar resonance frequencies can be lifted (Grage et al., 2001b).

The ^{19}F CSA tensors of various fluoro-benzene derivatives have been previously characterized by solid state NMR on single crystals (Nehring and Saupe, 1970; Hiyama et al., 1986; Griffin et al., 1973; Mehring, 1983) and in a model peptide (Grage et al., 2001b). According to these studies, the δ_{22} tensor component of the ^{19}F-substituent on an aromatic ring is aligned along the C–F bond (Figure 4) and gives rise to the peak at intermediate chemical shift position of the static powder spectrum. The δ_{11} component lies in the plane of the aromatic ring and corresponds to the low field edge of the spectrum, while the δ_{33} component is perpendicular to the plane of the ring and corresponds to the high field edge of the spectrum. The chemical shift of any particular CSA orientation depends on two angles α and β which are equivalent to Euler angles in describing the relationship between the principal axis system of the ^{19}F CSA tensor and the laboratory frame defined by the static magnetic field direction $\mathbf{B_0}$:

$$\delta(\alpha,\beta) = \delta_{11}\cos^2\alpha\sin^2\beta + \delta_{22}\cos^2\beta + \delta_{33}\sin^2\alpha\sin^2\beta. \quad (2)$$

Here α is the angle of rotation about the C–F axis that would turn the plane of the phenyl ring into the plane defined by the $\mathbf{B_0}$ and C–F vectors, while β is the angle enclosed between the C–F vector (representing the δ_{22} component) and $\mathbf{B_0}$ (Figure 4A). In general, solutions for α and β can be obtained by analyzing the spectral lineshapes of oriented samples aligned at different tilt angles with respect to the magnetic field (Grage et al., 2001b; Ulrich and Watts, 1993).

In a uniaxially oriented system, such as F-GS in DMPC bilayers, the most fundamental experiment is carried out with a horizontally aligned sample, such that the macroscopic sample normal $\mathbf{N}$ lies parallel to the static magnetic field direction $\mathbf{B_0}$ ($\tau = 0°$). In this unique situation, the CSA tensors of all labelled molecules are equivalent with respect to $\mathbf{B_0}$ and a single narrow resonance at δ^0 is selected from the full CSA width ($\Delta_{CSA} = \delta_{33} - \delta_{11}$). On the other hand, when the sample is tilted at any other angle ($\tau \neq 0°$), the CSA tensors will by distributed over a range of different orientations with respect to the magnetic field. Therefore, characteristic broad and complex lineshapes are expected for all sample orientations other than the horizontal one. Only when the peptide undergoes fast axial rotation about the membrane normal will the CSA tensor be averaged about the macroscopic sample axis and a single ^{19}F resonance will appear at all sample orientations. In this case, as the sample is tilted at an angle τ, a single resonance frequency δ^τ occurs at a well-defined position between the edges ($\delta_{||} = \delta_0$ and $\delta_\perp = \delta_{90}$) of the rotationally averaged CSA tensor ($\Delta_{CSA} = \delta_{||} - \delta_\perp$) at either side of the isotropic chemical shift δ_{iso}, according to:

$$\delta^\tau = \delta_{iso} + \Delta_{CSA}(3\cos^2\tau - 1)/3 \quad (3)$$

Note that the axially averaged situation is expected to be observed for small peptides in liquid crystalline lipids but not in gel state lipids.

The first step in the proposed structure analysis will be to determine the ^{19}F CSA tensor orientation of a 4F-Phg labelled peptide in the laboratory frame by measuring a tilt-series of oriented membranes in the gel phase. As a second step, the CSA orientation (given by α and β) can then be used to find out how the peptide backbone of a given secondary structure element is aligned with respect to the membrane plane. Such a coordinate transformation into the molecular frame, however, requires knowledge of the local side chain torsion angle χ_1 around the C_α–C_β bond of 4F-Phg (Figures 4B and 5A). The orientation of the C_ε–F bond corresponds directly to the δ_{22} tensor component, but the δ_{11} and δ_{33} components vary with the value of χ_1. In general, χ_1 depends mainly on the local backbone conformation, as the side chain C_γ–H groups tend to avoid repulsive interactions with the C_{i-1}=O_{i-1}, N_i–H_i, C_i=O_i and N_{i+1}–H_{i+1} peptide groups (Chandrasekaran and Ramachandran, 1970; Gelin and Karplus, 1979; Dunbrack and Karplus, 1994). The case of a phenylglycine residue is rather special, because the two C_γ atoms in the aromatic ring are attached to a branched C_β that is trigonal-planar instead of tetrahedral. In order to predict the preferred conformation of 4F-Phg, we carried out a conformational analysis on a model *N*-acetyl-*N′*-methylamide dipeptide derivative of this residue. Using molecular mechanics, the torsion angle χ_1 of the 4F-Phg side-chain was varied from 0° to 180° and the total energy was calculated (Figure 5). For backbone conformations typical of β-sheets (ϕ between $-60°$ and $-180°$, and ψ between 30° and 180°), the energy profile shows a single minimum at $\chi_1 = 60° \pm 10°$. Using the backbone conformation of 4F-Phg

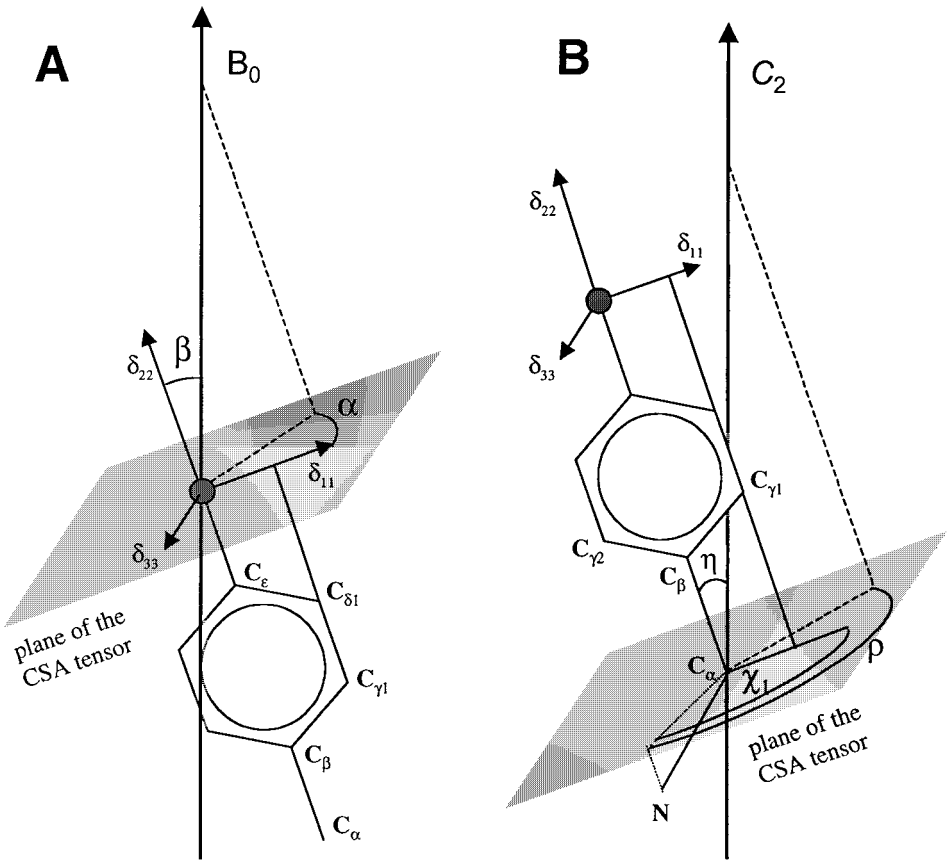

Figure 4. Assignment of the principal components of the ^{19}F CSA tensor in 4F-Phg, and definition of the angles used in this study. (A) The Euler angles α and β describe the CSA tensor in the laboratory frame and are defined with respect to the direction of the $\mathbf{B_0}$ magnetic field. (B) The angles η, χ_1 and ρ refer to the molecular coordinate system of any molecule, and in the case of F-GS they are defined with respect to the C_2 symmetry axis. When the three axis, $\mathbf{B_0}$, **N** and C_2 are parallel, then $\eta = \beta$, and $\alpha = (\chi_1 - \rho)$.

in our model F-GS structure ($\phi = -145.9°$, $\psi = 78.3°$), which is taken to be the same as in natural GS (Xu et al., 1995), we find a minimum at $\chi_1 = 55°$ (Figure 5B). This energy profile reveals two important aspects about the expected behaviour of 4F-Phg. First, the curve is asymmetrically centered around a single minimum, corresponding to values of $35° < \chi_1 < 60°$, having energy values within 1 kcal/mol from the most stable conformation. Second, conformations in the region between $90° < \chi_1 < 150°$ are strongly disfavoured due to a direct steric clash between C_γ–H and the peptide carbonyl group. This means that free ring rotation is not expected in the rigid β-sheet backbone, even at high temperature.

Alignment of F-GS in DMPC bilayers

The solid state ^{19}F-NMR spectra of a non-oriented dispersion and of a uniaxially oriented sample of F-GS in hydrated DMPC bilayers at an 80:1 lipid:peptide molar ratio are shown in Figure 6. The corresponding experimental chemical shift values are summarized and evaluated further in Table 2. Analogous results were obtained for a 200:1 lipid:peptide ratio (not shown). The data of F-GS recorded at 0 °C correspond to the gel phase of the lipid (Figure 6A-C). Here, the powder spectrum extends over approximately 90 ppm and shows the typical features of a static ^{19}F CSA tensor with an asymmetry parameter of about 0.54 (Figure 6A). The principal axis values, δ_{11}, δ_{22}, δ_{33} are close to the literature values of related compounds (Grage et al., 2001b; Nehring and Saupe, 1970). These findings indicate that there is no significant motion in the molecule which would otherwise lead to an averaging of the CSA tensor. When the oriented sample of F-GS is aligned horizontally with respect to the magnetic field ($\tau = 0°$), the spectrum shows a single, relatively broad feature at $\delta^0 \approx -124$ ppm

Table 2. Experimental and calculated parameters for the ^{19}F-CSA of F-GS in DMPC. The effects of peptide rotation and peptide wobble are evaluated in order to correlate the experimental data of the gel state with that of the liquid crystalline phase (see Discussion). All chemical shift values are given in ppm, and the numbers in brackets are estimated errors.

Successive motional states		$[\delta^0]^a$	δ_{11}	δ_{22}	δ_{33}	δ^b_{iso}	$\delta_\perp$	$\delta_\parallel$	Δ^c_{CSA}
Experimental Immobile gel phase[d]		−124.0 (0.5)	−65.5 (0.5)	−126.5 (0.5)	−153.0 (0.5)	−115.0 (0.5)			88.5 (0.5)
Calculated	+ Peptide rotation	−124.0 (0.5)				−115.0 (0.5)	−110.5 (0.5)	−124.0 (0.5)	13.5 (0.5)
	+ Peptide rotation + Peptide wobble[e]	−118.1 (0.5)				−115.0 (0.5)	−113.4 (0.5)	−118.1 (0.5)	4.7 (0.5)
Experimental Liquid crystalline phase[f]		−118.05[g] (0.2)				−115.0 (0.2)	−113.5 (0.2)	−118.05[g] (0.2)	4.55 (0.2)

[a]Chemical shift at $\tau = 0°$ tilt.
[b]Isotropic chemical shift, given by the average $(\delta_{11} + \delta_{22} + \delta_{33},)/3$, or $(2\delta_\perp + \delta_\parallel./3$.
[c]Total width of the CSA tensor, given by the difference $\delta_{33} - \delta_{11}$, or $\delta_\parallel - \delta_\perp$.
[d]Data measured at 0 °C.
[e]Remaining order parameter $S_{mol} = 0.35$.
[f]Data measured at 30 °C, showing a partially resolved homonuclear dipolar splitting at ($\tau = 0°$).
[g]Average frequency of the line that is split by ^{19}F-^{19}F dipolar coupling.

(Figure 6B). When the sample is tilted to the vertical alignment ($\tau = 90°$), a more complex lineshape is observed (Figure 6C), which covers the same bandwidth as the powder spectrum. This behaviour is completely consistent with a lack of peptide rotation in the bilayer, as expected for the lipid gel phase.

In the liquid crystalline state at 30 °C, the powder spectrum is rather narrow, covering a width of about 4 ppm (Figure 6D), and the oriented sample shows even sharper features. When the oriented membranes are aligned horizontally ($\tau = 0°$), the ^{19}F-signal appears with a slight splitting at the high-field edge of the powder spectrum, namely at $\delta^0 = -117.8/118.3$ ppm (Figure 6E). At the vertical sample orientation ($\tau = 90°$), the signal moves to the corresponding low-field edge (Figure 6F). Additional sample tilt angles measured between $\tau = 0$ and 90° (data not shown) revealed a smooth shift of the resonance line, proportional to $(3\cos^2\tau - 1)/2$. This axially symmetric behaviour of the oriented sample indicates that at 30 °C the peptide is rotating fast about the membrane normal, and there may be additional motions leading to further signal averaging. Note that a slight splitting of about 0.5 ± 0.1 ppm is visible in the spectrum of the horizontally aligned sample (Figure 6E), which is at the limit of resolution but was repeatedly observed in different samples. This splitting corresponds to 200–300 Hz and represents the same homonuclear dipolar ^{19}F-^{19}F coupling of 270 Hz that was measured above in the CPMG spectrum of Figure 3C with much higher accuracy. The mean chemical shift of this doublet corresponds to 118.05 ppm, which will be used in the further analysis and in Table 2.

To take a shortcut in the structural interpretation of how the peptide is aligned in the membrane, we will now make use of some symmetry considerations. In general, a horizontally aligned sample containing a peptide with two distinct 4F-Phg side chains in different orientations should give rise to two separate ^{19}F-NMR resonances. In the cyclic F-GS molecule, however, the two ^{19}F-substituents are related to one another by a C_2 symmetry axis (see Figure 1), with which they form an angle η (Figure 4B). Provided that the two side chains are aligned at different angles with respect to the membrane normal, two different signals would be expected. However, the observed spectra (Figures 6B and 6E) show that the two ^{19}F-labels have identical resonance positions ($\delta^0 \approx -124$ ppm at 0°, and $\delta^0 = -118.05$ ppm at 30 °C when taking the homonuclear dipolar splitting into account).

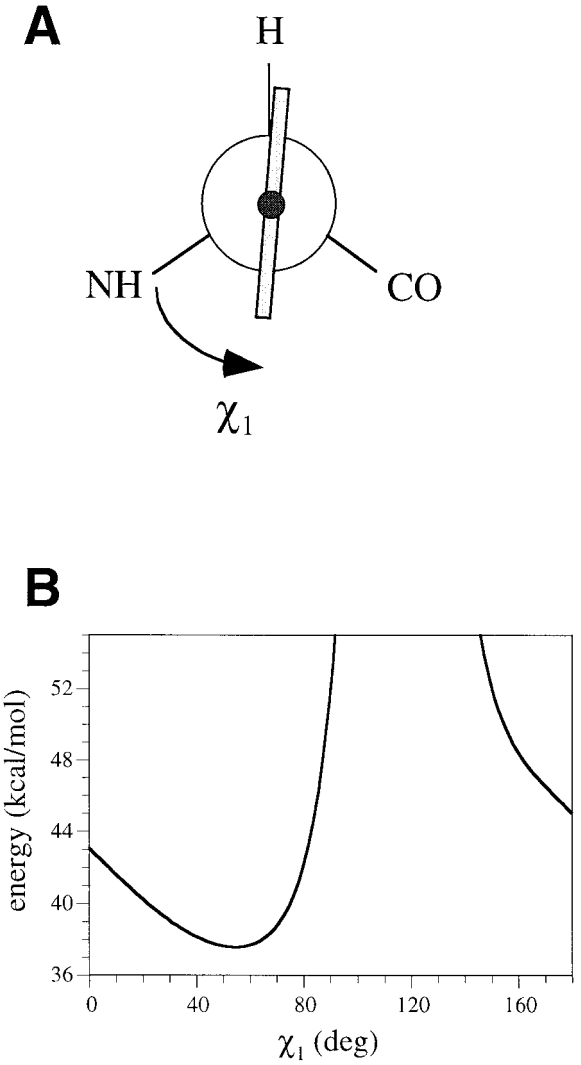

Figure 5. (A) Definition of the torsion angle χ_1 in the 4F-Phg side chain (Neuman projection). (B) Conformational analysis of the model compound *N*-acetyl-*N'*-methylamide-4-fluoro-phenylglycine. The total energy was calculated as a function of the torsion angle χ_1 in the 4F-Phg side chain using molecular mechanics. The values of $\phi = -145.9°$ and $\psi = 78.3°$ were taken from the backbone conformation of 4F-Phg in our model structure of F-GS. Note the asymmetry of the curve around the minimum and the sterically non-allowed conformations for $90° < \chi_1 < 150°$.

Therefore, on the assumption that the two 4F-Phg side chains possess the same torsion angle χ_1, the two C_ε–F bonds must be aligned at the same orientation with respect to the bilayer normal. This is the case when the symmetry axis C_2 of the F-GS molecule is aligned parallel to the bilayer normal, namely when the β-sheet backbone of the peptide lies flat in the plane of the membrane, as illustrated in Figure 7.

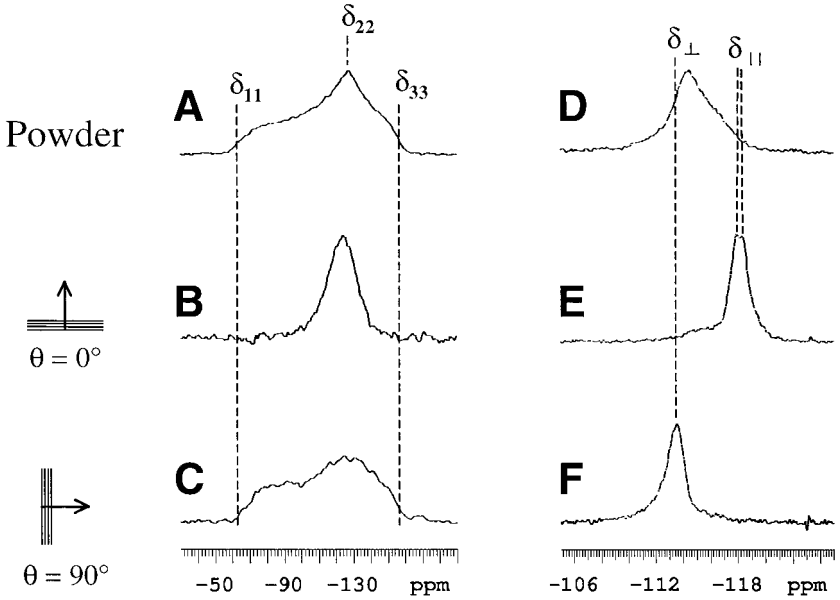

Figure 6. ^{19}F-NMR spectra of a hydrated mixture of F-GS in DMPC with a lipid:peptide molar ratio of 80:1, measured in the gel state (0 °C, A-C) and in the liquid crystalline phase (30 °C, D-F). A and D are powder spectra (see the Discussion and Figure 4A for an assignment of the CSA tensor components). B and E are spectra of oriented samples placed horizontally into the static magnetic field (with the sample normal aligned parallel to the field, $\tau = 0°$). C and F are spectra of oriented samples aligned vertically (sample normal at right angle to the field, $\tau = 90°$). The small splitting in spectrum E corresponds to the homonuclear dipolar ^{19}F-^{19}F coupling that has been well resolved by the CPMG experiment in Figure 3C. Note the different frequency scales for spectra A-C and for spectra D-F.

The conceptually simple proposal of a flat peptide orientation based on symmetry arguments can now be verified by calculating the ^{19}F chemical shifts that would be expected for such alignment of F-GS in the membrane. First, consider the sample in the gel phase (Figure 6A–C), with the F-GS peptide positioned accordingly into the lipid bilayer. When the sample is aligned horizontally, the molecular symmetry axis C_2, the sample normal **N**, and the magnetic field direction $\mathbf{B_0}$ coincide. Therefore, β equals η, and α is related to χ_1 according to $\alpha = (\chi_1 - \rho)$, as illustrated in Figure 4. Note that α is zero when $\mathbf{B_0}$ (given by the plane C_β–C_γ–C_δ) lies in-plane with the aromatic ring, whereas χ_1 is defined to be zero when the C_α–N bond lies in-plane with the aromatic ring (Figures 4A, 4B and 5A). To relate α with χ_1 (for the case that C_2 and $\mathbf{B_0}$ are parallel), we have introduced here the parameter ρ, which is the angle formed between the projections of the C_α–N vector and the symmetry axis C_2 onto a plane perpendicular to the C_α–C_β vector (Figure 4B). In our model structure of F-GS we find that $\rho = 55°$, $\eta = 172°$ and $\chi_1 = 55°$. Since in our case ρ and χ_1 happen to have the same numerical value, this makes $\alpha = 0°$. Based on these values, we can now calculate the expected resonance frequency δ^0 from the static CSA tensor values of Figure 6A (Table 2) using Equation 2. The predicted result of -125.3 ppm $\pm$ 0.5, is in excellent agreement with the experimental value of -124 ppm (Figure 6B), within 2% error of the total accessible CSA range of 90 ppm.

Despite the excellent agreement between experiment and prediction, we will need to assess by how much the real structure of F-GS can deviate from the starting model used here while still being compatible with our data. For example, the backbone conformation of the analogue GS(KY) discussed above (see Figure 3) leads to a value of $\eta = -146°$, instead of 172° for the native GS. Additionally, the 4F-phenylglycine torsion angle χ_1 could vary around its energy minimum of 55° (see above and Figure 4). In view of these potential sources of error, we will now examine how the ^{19}F resonance frequency would depend on η and χ_1 if these angles were allowed to change freely. This analysis is carried out in the most general way by sweeping the CSA tensor through the entire orientational space spanned by the two Euler angles α and β. The 3D contour-plot in Figure 8A shows the expected ^{19}F chemical shift value as a function of α and β for a horizontally aligned sample ($\tau = 0°$), calculated according to Equation 2 and under the as-

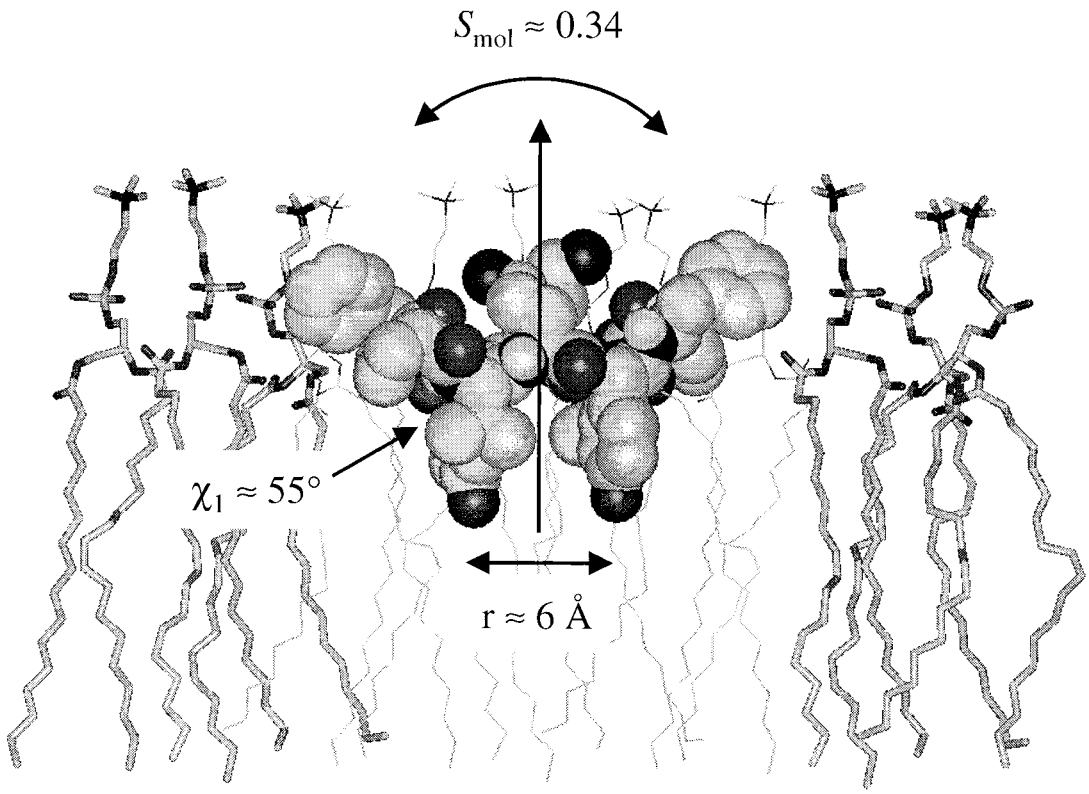

Figure 7. Proposed structure and flat alignment of F-GS in liquid crystalline DMPC bilayers for lipid:peptide molar ratios between 80:1 and 200:1. The values for the ^{19}F-^{19}F distance r, for the molecular order parameter S_{mol}, and for the 4F-Phg side chain torsion angle χ_1 were determined as a self-consistent solution from the solid state ^{19}F-NMR data.

sumption that there is no motional averaging (which is justified in the lipid gel phase). The projection map (Figure 8B) displays all combinations of α and β that are compatible within error margins with the experimentally observed chemical shift ($\delta_0 = -124$ ppm ± 0.5) measured at a horizontal sample tilt in the lipid gel phase (Figure 6B, Table 2). The plot is symmetrical around $\alpha = 0°$ and $\beta = 90°$ due to the $\cos^2$ and $\sin^2$ terms of Equation 2, which means that mirror images cannot be structurally distinguished. Furthermore, as a result of the quasi-rectangular shape of the projection map, it turns out that a rather large uncertainty is associated with the value of α when β is well-defined and *vice versa*. This means that there exist regions where either α or β, but not both parameters simultaneously, can be precisely defined, namely in the regions near $\alpha = \pm 55°$ (horizontal bands in the plot), and near $\beta = 10$–$15°$ and 165–170° (vertical bands in the plot), respectively. If we want to discuss this general map in terms of the specific structural parameters of gramicidin S, namely in terms of $\chi_1 = (\alpha + \rho)$ and $\eta = \beta$, we have to keep in mind that any strong deviation in η from the structure of our starting model may necessitate a re-evaluation of ρ, because this angle is defined in relation to the framework of the given peptide structure. However, this latter concern only affects the regions of low definition of β (and η) in the plot, where the peptide backbone is ill-defined but χ_1 is well defined (at $\alpha = \pm 55°$, $\chi_1 = \pm 55° + \rho$). At this point it is important to realize that these awkward horizontal bands in the plot can be discarded anyway, for two reasons: First, the corresponding values of η deviate too much from a reasonable structure of the peptide because they are too small for an antiparallel β-sheet backbone conformation. Second, the corresponding χ_1 rotamers in this region are sterically highly unlikely (see above and Figure 5), even if we allow for a ±20° deviation of ρ with respect to the value taken from our model structure ($\rho = 55°$). On the other hand, if we consider the region of $\beta = 165°$–170° (shaded box in Figure 8B), this vertical band is consistent with a well-defined antiparallel β-sheet structure with $\eta = 165°$–170°, which is very close to the structure of native GS (Xu et al., 1995) and to our

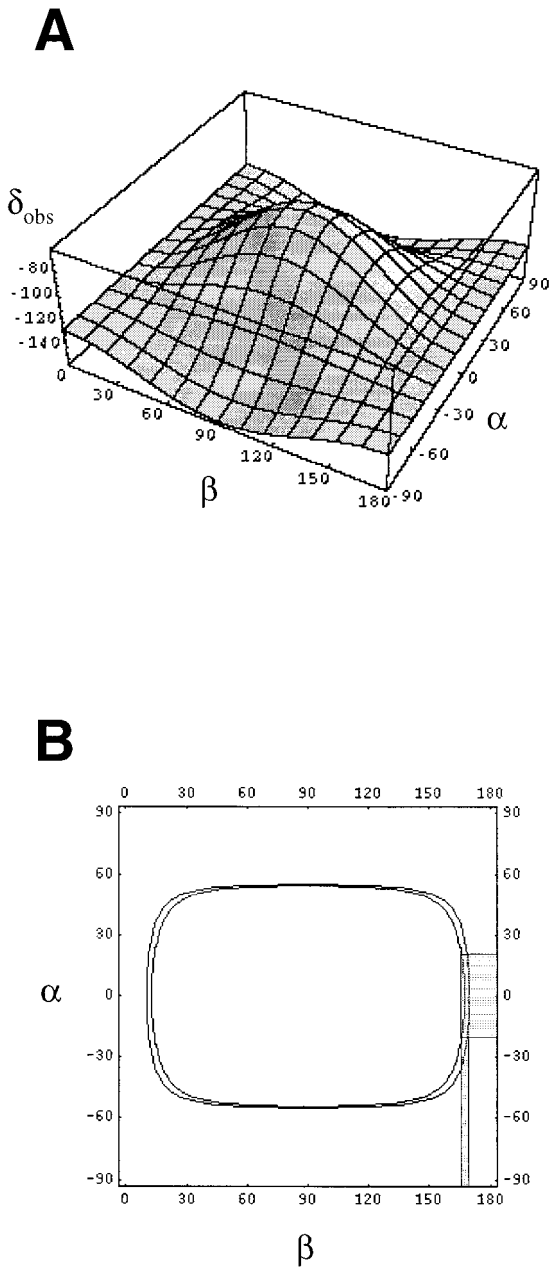

Figure 8. (A) Predicted values of the ^{19}F chemical shift δ(α,β) calculated according to Equation 2 as a function of the Euler angles α and β, based on the experimental analysis of the CSA tensor of F-GS (Figure 6A, Table 2). (B) Projection map corresponding to the observed chemical shift in the horizontally aligned sample at 0 °C ($\delta^0 = -124$ ppm ± 0.5). The shaded boxes in the plot correspond to the structural parameters $\eta = \beta = 170 \pm 5°$ and $\chi_1 = (\alpha + \rho) = 55 \pm 20°$ that were independently derived to support our proposed model of F-GS.

model structure of F-GS ($\eta = 172°$). In this sterically accessible range of backbone and side chain torsion angles, and within the experimentally allowed range of α values in the plot ($\alpha = 0° \pm 20°$), we obtain a result for χ_1 that is centred around $\chi_1 = (\alpha + \rho) = 55°$. This experimental result is in excellent agreement with the most favourable rotamer that had been independently predicted by energy minimization (Figure 5).

To summarize, we have performed the search through Euler space (Figure 8) without any initial structural assumptions, and we used only some stringent sterical arguments to dismiss a certain range of solutions from the allowed regions in the plot. As a result, the ^{19}F-NMR data are fully consistent with values of $\eta = 170° \pm 5°$ and $\rho = 55° \pm 5°$. These parameters, which should correspond to the structure of F-GS in the lipid membrane, are in good agreement with our starting model of this peptide based on the backbone conformation of the natural GS in solution. Thus, it seems that the substitution of Leu by 4F-Phg does not affect significantly the backbone structure of GS, just as we had initially assumed. Concerning the 4F-Phg side-chain torsion angle, the value of χ_1 is found to be around 55° and compatible with the NMR data within an error of ±20°. Since the conformational energy for 4F-Phg was found to be asymmetrically centered around a steep minimum (Figure 5B), the range of allowed values of χ_1 can be reasonably set from 40° to 60°.

Dynamic behaviour of F-GS in DMPC bilayers

In liquid crystalline membranes at high temperature, the relatively narrow powder spectrum of F-GS and the pattern of the corresponding oriented samples show that the ^{19}F CSA tensor is axially averaged about the membrane normal (see Table 2). When compared to the spectra in the gel phase, an overall peptide rotation alone would not change the line position δ^0 in the horizontally aligned sample ($\tau = 0°$). However, it is seen from Figure 6 that the resonance moves from −124 ppm at 0 °C to 118.05 ppm at 30 °C, which must be attributed to the onset of further modes of motional averaging. A whole-body wobbling motion of the peptide can be described by a molecular order parameter S_{mol} = (4.55 ppm/13.5 ppm) = 0.34 ± 0.05, which is calculated from the CSA tensor widths, Δ_{CSA}, as the ratio of the CSA width measured at 30 °C over the theoretical CSA width for peptide rotation only, as listed in Table 2. The order parameter is defined as the time average over $<3\cos^2\sigma(t) - 1>/2$, where

σ(t) is the time-dependent angle between the molecular symmetry axis C_2 of F-GS and the membrane normal **N**. According to the simplest wobble-within-a-cone model, it is estimated that σ changes as much as ±40° due to the peptide wobble.

In an alternative motional model, an additional ring-flip on the 4F-phenyl group around the C_α–C_β bond may be considered. This kind of motion would already reduce the effective width of the CSA powder spectrum to 17.5 ppm, and any further narrowing due to long-axial peptide rotation would then only contribute an additional narrowing factor of $[3\ \cos^2(172°) - 1]/2 = 0.97$. The latter model would thus yield an oder parameter of $S_{mol} = (4.55\ ppm/17.0\ ppm) = 0.27$. From the current NMR data alone we cannot draw a final conclusion about the side chain dynamics and cannot decide which of the two side chain motional models applies, although we expect from our conformational energy calculation above that a ring rotation of 4F-Phg is sterically unfavourable. Nevertheless, in either case it is obvious that the small peptide is highly mobile when bound to the lipid bilayer in the liquid crystalline phase, whereas it is virtually immobilized in the gel state.

Self-consistent solution for all structural parameters

Figure 7 summarizes the picture of F-GS as it is accommodated in liquid crystalline lipid bilayers, based on the three inter-related structural parameters that we have determined by solid state ^{19}F-NMR. The flat alignment of the peptide backbone was deduced from the occurrence of a single resonance line and confirmed by an *ab initio* analysis of the Euler space, which also yielded a 4F-Phg torsion angle of $\chi_1 \approx 55°$. The order parameter $S_{mol} = 0.34 \pm 0.05$ (or 0.27±0.05, depending on whether side chain rotation is assumed or not) was evaluated from the temperature-dependent shift of the resonance line upon passing through the lipid phase transition. This dynamic averaging factor may now be used to refine the intramolecular distance between the two ^{19}F-labels from their dipolar coupling. For this purpose, the splitting $\Delta_{FF} = 270$ Hz in the CPMG spectrum of Figure 3C has to be multiplied by (i) the order parameter S_{mol} and by (ii) the geometric factor $(3\cos^2\theta - 1)/2$ according to Equation 1. Since we have shown above that the internuclear ^{19}F-^{19}F vector is aligned at right angle with respect to the membrane normal **N**, the geometric factor is equal to $-1/2$. Using these two multiplication factors, the internuclear distance is calculated to be $r \approx 6$ Å, with an estimated accuracy of about 1 Å. Especially the value of the order parameter S_{mol}, nominally between 0.22 and 0.39 (depending on the assumption of any side chain rotation), is the most significant source of error in this iterative analysis, hence we attributed a generous error range to the evaluation of r. This ^{19}F-^{19}F distance of 6 ± 1 Å is close to the value expected from the structure of native gramicidin S in solution (7.3 Å, see the model structure in Figure 7A), while it is far from the distorted structure of the corresponding GS(KY) analogue (Figure 7B). The close similarity between our F-GS results and the native peptide in solution suggests that the structure of gramicidin S does not change significantly upon 4F-Phg labelling, nor upon binding of the peptide to the DMPC membrane.

Conclusions

We have determined the alignment and the dynamics of an antimicrobial cyclic β-sheet peptide derivative of gramicidin S in DMPC bilayers, both in the lipid gel state and in the liquid crystalline phase. Additionally we have determined valuable distance and angular constraints, which have allowed us to propose a realistic model of the peptide bound to the lipid membrane, and to demonstrate that this structure is very similar to natural GS in solution. By observing a selectively ^{19}F-labelled analogue with two equivalent 4F-phenylglycine side chains, we have measured (i) an intramolecular ^{19}F-^{19}F distance of 6 ± 1 Å, (ii) the orientations of the C_ε–F vectors with respect to the membrane normal, and (iii) the side-chain torsion angle of the 4F-Phg residues. The high sensitivity of ^{19}F-NMR allowed the characterization of as little as 0.2 mg peptide (0.16 μmol) in relatively short acquisition times (1 to 7 h, depending on the phase state of the lipids). The F-GS peptide is found to be oriented such that its cyclic β-sheet backbone lies flat in the plane of the membrane, which is fully consistent with the amphiphilic character of the molecule. It is reasonable to conclude that the peptide must be positioned at the bilayer/water interface, such that the polar side chains point towards the lipid head-groups while the hydrophobic residues intercalate between the lipid hydrocarbon chains. The relatively rigid secondary structure and the C_2 symmetry of the cyclic peptide seem to be conserved upon binding to the membrane, since the two 4F-Phg groups are oriented at the same angle with respect to the membrane normal, and their

distance is close to the one expected from the known backbone structure of native gramicidin S in solution. While the membrane-associated peptide is observed to be immobilized in the gel state, it becomes highly mobile in the fluid membrane and exhibits fast rotation around the bilayer normal and further wobbling with an order parameter of ~ 0.34.

This study represents the first direct observation of an antimicrobial β-sheet peptide in its membrane-associated state, and it illustrates one of the very first applications of solid state ^{19}F-NMR to a membrane-bound peptide. The experimentally derived picture of F-GS fully supports the expected behaviour of amphiphilic peptides in biological membranes at low peptide/lipid ratios, and it is in excellent agreement with recent molecular dynamics simulations of GS in a DMPC bilayer (Mihailescu and Smith, 2000). It will be interesting to extend this NMR study to other experimental conditions, as we have noticed a remarkably different orientational behaviour of F-GS at higher peptide concentration. Now that the properties of the 4F-Phg side chain have been evaluated both experimentally and theoretically in this initital study, the same ^{19}F-NMR approach may also be applied to any other membrane-active peptide that can be suitably labelled.

Acknowledgements

The authors gratefully acknowledge the EMBO foundation for a long-term fellowship for J.S., and the Deutsche Forschungsgemeinschaft for providing support within the SFB 197 (TP B13, A.S.U., S.L.G.). L.H.K., R.S.H., and R.N.M gratefully acknowledge support from the Protein Engineering Network of Centres of Excellence. We also thank Sergii Afonin, Ralf Glaser, and Ulrich Dürr for constructive discussions.

References

Adler, A.J.N., Greenfield, J. and Fasman, G.D. (1973) *Meth. Enzymol.*, **27**, 675–735.

Bechinger, B. (1999) *Biochim. Biophys. Acta*, **1462**, 157–183.

Chandrasekaran, R. and Ramachandran, G.N. (1970) *Int. J. Protein Res.*, **2**, 223–233.

Danielson, M.A. and Falke, J.J. (1996) *Annu. Rev. Biophys. Biomol. Struct.*, **25**, 163–95.

Datema, K.P., Pauls, K.P. and Bloom, M. (1986) *Biochemistry*, **25**, 3796–3803.

Davis, J.H. and Auger, M. (1999) *Prog. Nucl. Magn. Reson. Spectros.*, **35**, 1–84.

de Groot, H.J.M. (2000) *Curr. Opin. Struct. Biol.*, **10**, 593–600.

Dunbrack, R.L. and Karplus, M. (1994) *Nature Struct. Biol.*, **1**, 334–340.

Fu, R.Q. and Cross, T.A. (1999) *Annu. Rev. Biophys. Biomol. Struc.*, **28**, 235–268.

Gelin, B.R. and Karplus, M. (1979) *Biochemistry*, **18**, 1256–1268.

Gerig, J.T. (1994) *Prog. NMR Spectrosc.*, **26**, 291–370.

Gerig, J.T. (1998) *Online Biophysics Textbook*, Ed. V. Bloomfield, http://biosci.umn.edu/biophys/OLTB/Textbook.html.

Gibbs, A.C., Kondejewski, L.H., Gronwald, W., Nip, A.M., Hodges, R.S., Sykes, B.D. and Wishart, D.S. (1998) *Nat. Struct. Biol.*, **5**, 284–288.

Gilchrist, M.L., Monde, K., Tomita, Y., Iwashita, T., Nakanishi, K. and McDermott, A.E. (2001) *J. Magn. Res.*, **152**, 1–6.

Goetz, J.M., Poliks, B., Studelska, D.R., Fischer, M., Kugelbrey, K., Bacher, A., Cushman, M. and Schaefer, J. (1999) *J. Am. Chem. Soc.*, **121**, 7500–7508.

Grage, S.L. and Ulrich, A.S. (1999) *J. Magn. Reson.*, **138**, 98–106.

Grage, S.L. and Ulrich, A.S. (2000) *J. Magn. Reson.*, **146**, 81–88.

Grage, S.L., Gauger, D., Selle, C., Pohle, W., Richter, W. and Ulrich, A.S. (2000) *Phys. Chem. Chem. Phys.*, **2**, 4574–4579.

Grage, S.L., Salgado, J., Dürr, U., Afonin, S., Glaser, R.W. and. Ulrich, A.S. (2001a) In *Perspectives on Solid State NMR in Biology* (Eds. Kiihne, S.R. and De Groot, H.J.M.), Kluwer Academic Publishers, Dordrecht, pp. 38–91.

Grage, S.L., Wang, J., Cross, T.A. and Ulrich, A.S. (2001b) *J. Am. Chem. Soc.*, submitted.

Griffin, R.G., Yeung, H.N., LaPrade, N.D. and Waugh, J.S. (1973) *J. Chem. Phys.*, **59**, 777–783.

Gröbner, G., Burnett, I.J., Glaubitz, C., Chio, G., Mason, A.J. and Watts, A. (2000) *Nature*, **405**, 810–813.

Gu, Z.T.T. and Opella, S.J. (1999) *J. Magn. Reson.,* **140**, 340–346.

Harris, R.K. and Jackson, P. (1991) *Chem. Rev.*, **91**, 1427–1440.

Hiyama, Y., Silverton, J.V., Torchia, D.A., Gerig, J.T. and Hammond, S.J. (1986) *J. Am. Chem. Soc.*, **108**, 2715–2723.

Hull, S.E., Karlsson, R., Main, P., Woolfson, M.M. and Dodoson, E.J. (1978) *Nature,* **275**, 206–207.

Kahn, P.C. (1979) *Meth. Enzymol.,* **61**, 339–378.

Kondejewski, L.H., Farmer, S.W., Wishart, D.S., Hancock, R.E. and Hodges, R.S. (1996a) *Int. J. Pept. Protein Res.*, **47**, 460–466.

Kondejewski, L.H., Farmer, S.W., Wishart, D.S., Kay, C.M., Hancock, R.E.W. and Hodges, R.S. (1996b) *J. Biol. Chem.*, **271**, 25261–25268.

Kondejewski, L.H., Jelokhani-Niaraki, M., Farmer, S.W., Lix, B., Kay, C.M., Sykes, B.D., Hancock, R.E.W. and Hodges, R.S. (1999) *J. Biol. Chem.*, **274**, 13181–13192.

Lewis, R.N.A.H., Prenner, E.J., Kondejewski, L.H., Flach, C.R., Mendelsohn, R., Hodges, R.S. and McElhaney, R.N. (1999) *Biochemistry*, **38**, 15193–15203.

Losonczi, J.A. and Prestegard, J.H. (1998) *Biochemistry* **37**, 706–716.

Losonczi, J.A., Tian, F. and Prestegard, J.H. (2000) *Biochemistry* **39**, 3804–3816.

Marassi, F.M. and Opella, S.J. (1998) *Curr. Opinion Struct. Biol.*, **8**, 640–648.

McInnes, C., Kondejewski, L.H., Hodges, R.S. and Sykes, B.D. (2000) *J. Biol. Chem.*, **275**, 14287–14294.

Mehring, M. (1983) *Principles of High Resolution NMR in Solids*, Springer-Verlag, New York, NY.

Mihailescu, D. and Smith, J.C. (1999) *J. Phys. Chem. B*, **103**, 1586–1594.

Mihailescu, D. and Smith, J.C. (2000) *Biophys. J.*, **79**, 1718–1730.

Miller, J.M. (1996) *Prog. NMR Spectrosc.*, **28**, 255–281.

Nehring, J. and Saupe, A. (1970) *J. Chem. Phys.*, **52**, 1307–1310.

Opella, S.J., Marassi, F.M., Gesell, J.J., Valentine, A.P., Kim, Y., Oblatt-Montal, M. and Montal, M. (1999) *Nat. Struct. Biol.*, **6**, 374–379.

Prenner, E.J., Lewis, R.N.A.H., Neuman, K.C., Grunner, S.M., Kondejewski, L.H., Hodges, R.S. and McElhaney, R.N. (1997) *Biochemistry*, **36**, 7906–7916.

Prenner, E.J., Lewis, R.N.A.H., Kondejewski, L.H., Hodges, R.S. and McElhaney, R.N. (1999a) *Biochim. Biphys. Acta*, **1417**, 211–223.

Prenner, E.J., Lewis, R.N.A.H. and McElhaney, R.N. (1999b) *Biochim. Biphys. Acta*, **1462**, 201–221.

Ramamoorthy, A., Wu, C.H. and Opella, S.J. (1999) *J. Magn. Reson.*, **140**, 131–140.

Sitaram, N. and Nagaraj, R. (1999) *Biochim. Biophys. Acta*, **1462**, 29–54.

Smith, S.O., Aschheim, K. and Groesbeek, M. (1996) *Quart. Rev. Biophys*., **29**, 395–449.

Ulrich, A.S. (2000) In *Encyclopaedia of Spectroscopy and Spectrometry* (Eds. Lindon, J., Tanter, G. and Holmes, J.), Academic Press, New York, NY, pp. 813–825.

Ulrich, A.S. and Watts, A. (1993) *Solid State NMR*, **2**, 21–36.

Ulrich, A.S., Heyn, M.P. and Watts, A. (1992) *Biochemistry*, **31**, 10390–10399.

Ulrich, A.S., Wallat, I., Heyn, M.P. and Watts, A. (1995) *Nature Struct. Biol.*, **2**, 190–192.

Ulrich, A.S., Watts, A., Wallat, I. and Heyn, M.P. (1994) *Biochemistry*, **33**, 5370–5375.

van Beek, J.D., Beaulieu, L., Schäfer, H., Demura, M., Asakura, T. and Meier, B.H (2000) *Nature*, **405**, 1077–1079.

van Rossum, B.J., Förster, H. and de Groot, H.J.M. (1997) *J. Magn. Reson.*, **124**, 516–519.

Waki, M. and Izumiya, N. (1990) In *Biochemistry of Peptide Antibiotics* (Eds. Kleinkaug, H. and van Doren, H.), Walter de Gruyter, Berlin, pp. 205–244.

Watts, A., Ulrich, A.S. and Middleton, D.A. (1995) *Mol. Membr. Biol.*, **12**, 233–246.

Wu, M., Maier, E., Benz, R. and Hancock, R.E.W. (1999) *Biochemistry*, **38**, 7235–7242.

Xu, Y., Sugár, I.P. and Krishna, R. (1995) *J. Biomol. NMR*, **5**, 37–48.